APL/JHU CF-2886

16 September 1960

Copy No. 38

A STUDY OF THE ENERGY CONTENT OF A PERFECT GAS BEHIND A SHOCK WAVE FORMED BY A BLUNT BODY MOVING AT HYPERSONIC SPEEDS

by

R. A. Makofski

THE JOHNS HOPKINS UNIVERSITY
APPLIED PHYSICS LABORATORY
Silver Spring, Maryland

Operating under Contract NOrd 7386 with the Bureau of Naval Weapons, Department of the Navy

THE JOHNS HOPKINS UNIVERSITY
APPLIED PHYSICS LABORATORY
SILVER SPRING MARYLAND

A STUDY OF THE ENERGY CONTENT OF A PERFECT GAS BEHIND A SHOCK WAVE FORMED BY A BLUNT BODY MOVING AT HYPERSONIC SPEEDS

by

R. A. Makofski

Introduction

The use of blunt-nosed bodies to alleviate the heat transfer problem of re-entry vehicles has been widely discussed (e.g., Ref. 1). For such a vehicle, the shock wave generated by the blunt nose creates extremely high temperatures in the fluid in the vicinity of the vehicle. These high temperatures and the consequent radiation produced provide a means of detection of ballistic missiles (Ref. 2). At the same time, however, because of the spatial extent of the bow shock, it is expected that a significant portion of the energy dissipated will appear as thermal energy of the surrounding atmosphere. This increase in the thermal energy of the wake of the missile, or rather is distribution, is of interest as it may form an area of significant dimensions for use in detection purposes. It is for this purpose that a simplified analysis of the energy content of a fluid behind a shock wave has been conducted. A set of energy coefficients is defined and the relation of these coefficients to the wave drag of a body is given. The analysis is limited to a thermally and calorically perfect gas.

Conversion of Energy Due to a Shock Wave

The bow shock wave of a re-entry missile served to convert kinetic energy of the body into thermal and potential energy of the surrounding gas. In addition, the boundary layer surrounding the missile and the base flow, including vorticity, etc., also dissipated energy. The latter is relatively small compared to the former at high altitudes, so that for the purposes of this study only, the effects of the bow shock are considered. The flow, except through the shock wave, is assumed to be isentropic. Using Figure 1, the change in enthalpy is defined by

$$h_2 - h_\infty = (h_1 - h_\infty) + (h_2 - h_1)$$

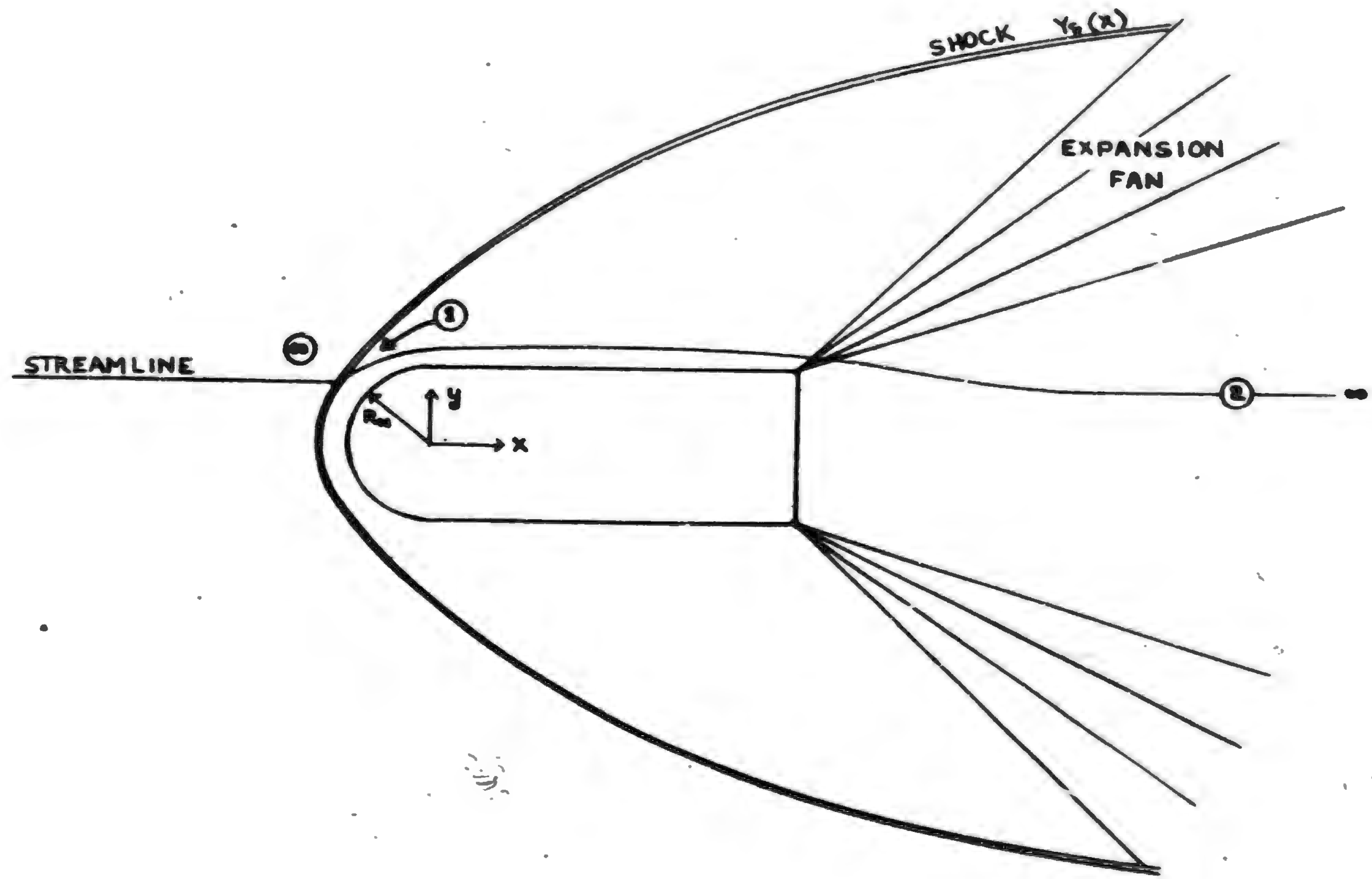

FIGURE 1 :. FLOW ABOUT AXI-SYMMETRIC BLUNT BODY

where h is the enthalpy per unit mass. For isentropic flow from Station 1 to 2,

$$\frac{h_2}{h_1} = \frac{T_2}{T_1} = \frac{P_2}{P_1}^{\frac{\gamma-1}{\gamma}},$$

where T represents absolute temperature and γ the ratio of specific heats. If Station 2 is far removed from the shock, $P_2 = P_\infty$. Then the change in enthalpy is given by

$$\frac{h_2}{h_\infty} - 1 = \left(\frac{h_1}{h_\infty} - 1\right) + \frac{h_1}{h_\infty}\left[\left(\frac{P_\infty}{P_1}\right)^{\frac{\gamma-1}{\gamma}} - 1\right] = \frac{h_1}{h_\infty}\left(\frac{P_\infty}{P_1}\right)^{\frac{\gamma-1}{\gamma}} - 1 \qquad (1)$$

The term

$$\frac{h_1}{P_1^{\frac{\gamma-1}{\gamma}}} \cdot \frac{P_\infty^{\frac{\gamma-1}{\gamma}}}{h_\infty} = \frac{P_{t_\infty}^{\frac{\gamma-1}{\gamma}}}{T_{t\infty}} \cdot \frac{T_{t1}}{P_{t1}^{\frac{\gamma-1}{\gamma}}} = \left(\frac{P_{t_\infty}}{P_{t1}}\right)^{\frac{\gamma-1}{\gamma}}$$

where the subscript t represents total or stagnation temperature and $T_{t1} = T_{t_\infty}$ across a shock wave. Therefore,

$$\frac{h_2}{h_\infty} - 1 = \left(\frac{P_{t_\infty}}{P_{t1}}\right)^{\frac{\gamma-1}{\gamma}} - 1 \qquad (2)$$

The change in the enthalpy of the entire flow field per unit time can be obtained by integrating equation (2) over the shock wave, i.e.,

$$H_2 - H_\infty = \int_{\Sigma_s} \rho_\infty U_\infty \sin\beta \, (h_2 - h_\infty) \, d\Sigma$$

where Σ_s is the shock surface area and $\beta = \tan^{-1} \frac{dy_s}{dx}$, i.e., the local shock wave angle.

Then

$$\frac{H_2 - H_\infty}{2 H_{n\infty}} = \int_0^\infty \left[\left(\frac{P_{t\infty}}{P_{t1}} \right)^{\frac{\gamma-1}{\gamma}} - 1 \right] \bar{y}_s \, d\bar{y}_s \tag{3}$$

where $\bar{y}_s$ is the shock height non-dimensionalized with respect to R_n, and $H_{n\infty} = \pi R_n^2 \rho_\infty U_\infty h_\infty$, i.e., the flux enthalpy into a normal shock of radius R_n. The total pressure ratio, $P_{t1}/P_{t\infty}$, may be expressed in terms of M_∞ and β by the relation

$$\frac{P_{t1}}{P_{t\infty}} = \left[\frac{(\gamma + 1) M_\infty^2 \sin^2\beta}{(\gamma - 1) M_\infty^2 \sin^2\beta + 2} \right]^{\frac{\gamma}{\gamma-1}} \left[\frac{\gamma + 1}{2\gamma M_\infty^2 \sin^2\beta - (\gamma - 1)} \right]^{\frac{1}{\gamma-1}}$$

To obtain a relation between $H_2 - H_\infty$ and the wave drag of a body, we define an enthalpy change coefficient due to the shock wave as

$$C_{H_w} = \frac{H_2 - H_\infty}{\pi R_n^2 \cdot \frac{1}{2} \rho_\infty U_\infty^3} = \frac{4}{(\gamma - 1) M_\infty^2} \int_0^\infty \left[\left(\frac{P_{t\infty}}{P_{t1}} \right)^{\frac{\gamma-1}{\gamma}} - 1 \right] \bar{y}_s \, d\bar{y}_s \tag{4}$$

In a similar manner, the internal energy may be expressed as

$$\frac{E_2 - E_\infty}{2 E_{n\infty}} = \frac{H_2 - H_\infty}{2 H_{n\infty}} \tag{5}$$

where $E_{n\infty} = \pi R_n^2 \rho_\infty U_\infty e_\infty$; $e_\infty = c_v T_\infty$

and

$$C_{E_w} = \frac{E_2 - E_\infty}{\pi R_n^2 (\frac{1}{2}\rho_\infty U_\infty^2)} = \frac{C_{H_w}}{\gamma} \qquad (6)$$

Relation of Enthalpy Change to Wave Drag

The wave drag of a body due to the momentum change across a shock wave has been derived by Munk and Crown (Ref. 3). Their relation for the wave drag coefficient is

$$C_{D_w} = \frac{D}{\pi R_n^2 (\frac{1}{2}\rho_\infty U_\infty^2)} = 4 \int_0^\infty \left(1 - \frac{u_2}{U_\infty}\right) \bar{y}_s \, d\bar{y}_s$$

This relation may also be written as

$$C_{D_w} = 4 \int_0^\infty \left\{ 1 - \left[1 - \frac{2}{(\gamma-1)M_\infty^2} \left\{ \left(\frac{P_{t\infty}}{P_{t1}}\right)^{\frac{\gamma-1}{\gamma}} - 1 \right\} \right]^{\frac{1}{2}} \right\} \bar{y} \, d\bar{y} \qquad (7)$$

Expanding the term in brackets using $\lambda = \left(\frac{P_\infty}{P_1}\right)^{\frac{\gamma-1}{\gamma}} - 1$

$$\left\{ 1 - \left[1 - \frac{2\lambda}{(\gamma-1)M_\infty^2} \right]^{\frac{1}{2}} \right\} = \frac{\lambda}{(\gamma-1)M_\infty^2} + \frac{\lambda^2}{2(\gamma-1)^2 M_\infty^4} + \cdot \; \cdot \; \cdot$$

If $\frac{\lambda}{2(\gamma-1)M_\infty^2} << 1$, then we need only use the first term of the expansion. In this case,

$$C_{D_w} \simeq \frac{4}{(\gamma-1)M_\infty^2} \int_0^\infty \left[\left(\frac{P_{t\infty}}{P_{t1}}\right)^{\frac{\gamma-1}{\gamma}} - 1 \right] \bar{y}_s \, d\bar{y}_s = C_{H_w} \qquad (8)$$

So, if $\frac{\lambda}{2(\gamma-1)M_\infty^2} << 1$, the wave drag coefficient is equal to the enthalpy change coefficient.

The maximum value of $\frac{\lambda}{2(\gamma-1)M_\infty^2}$ will occur for normal shock waves. As shown in Figure 2, this value does not exceed .07 for $\gamma \geqq 1.4$, and may be considered negligible for $M > 10$. This means that for $\gamma \geqq 1.4$, the enthalpy change coefficient and the wave drag coefficient are nearly equal. This condition may not be true for $\gamma < 1.4$.

The relation expressed in equation (8) allows a simplification in the computation of the change in enthalpy flux through a shock wave. At high Mach numbers ($M_\infty > 6$), the wave drag coefficient appears to remain constant (Ref. 4). This means that $H_2 - H_\infty$ may be expressed in terms of the Mach number and the enthalpy flux into a normal shock wave of radius, R_a, i.e.,

$$\frac{H_2 - H_\infty}{2 H_{a_\infty}} = \frac{(\gamma - 1)M_\infty^2}{4} C_{H_w} = K M_\infty^2 \tag{9}$$

where K = constant

Calculation of Enthalpy Change Through a Shock Wave

Shock Wave Shape: The change in enthalpy flux through a shock wave (Eq. 3) is a function of the Mach number and shock wave shape (or Mach number and body geometry). Unfortunately, the methods of computing the shock shape (e.g., method of characteristics) are laborious and experimental data is lacking. To avoid the lengthy computations, and since we are seeking only qualitative information, the shock wave shape for the semi-infinite hemisphere cylinder of Ref. 2 is used. This shock will differ from the shock that would occur at higher Mach numbers for a finite body. The effect of this difference on the results obtained will be discussed later.

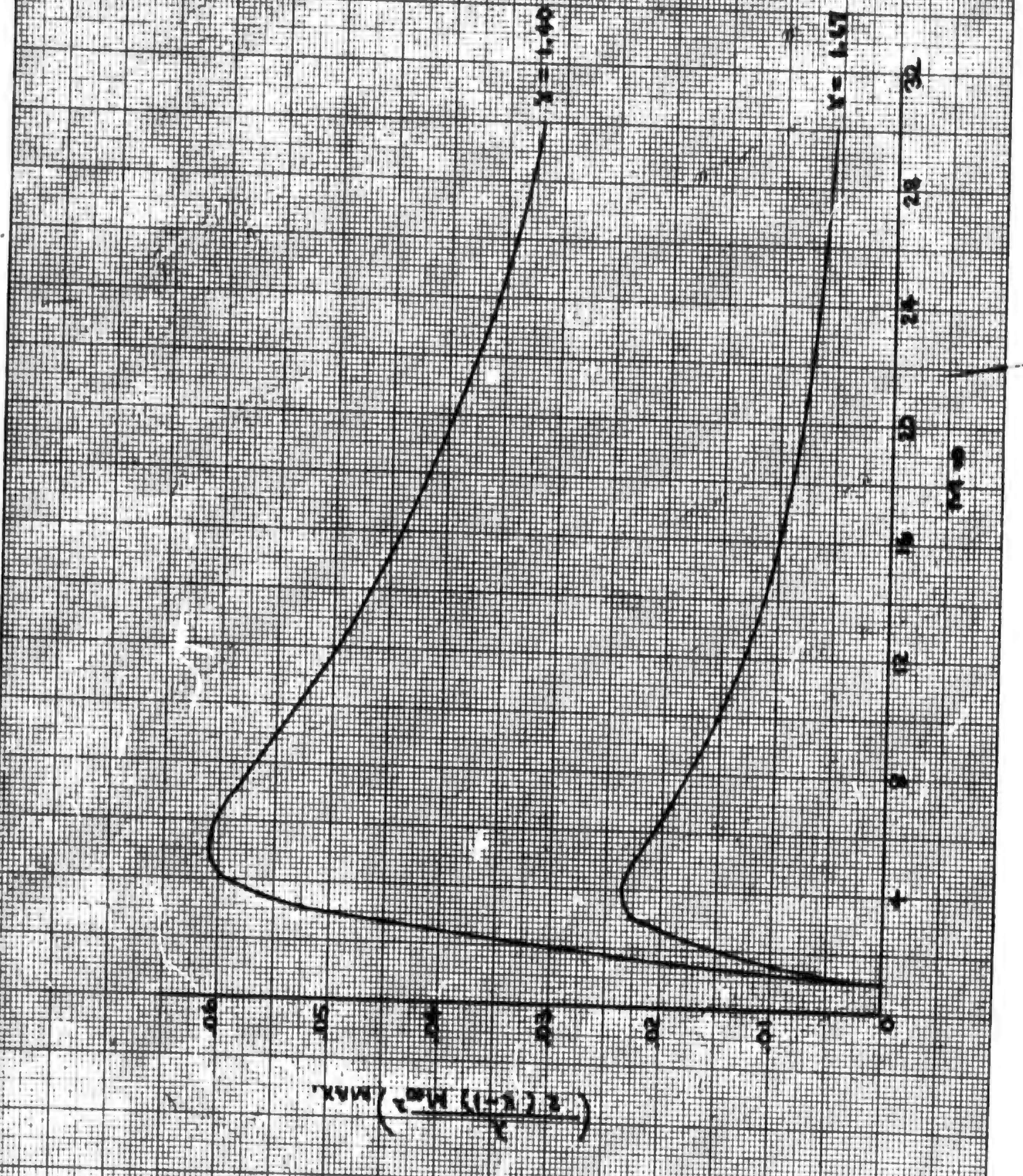

FIGURE 2 : MAXIMUM ERROR INVOLVED IN ASSUMING $C_{D_W} = C_{f_W}$

Of importance, also, is the fact that the shock shape of Ref. 2 does not extend to the Mach line. Thus, the missing portion of the curve must be taken into account in discussing the final results.

Calculation of Energy Change: For the above shock wave shape, the change in enthalpy flux has been computed as a function of $\bar{y}_s$ for $M_\infty = 20$ and 27.7 (Fig. 3a and 3b). In both cases, the shock shape is assumed to remain constant. This is justified as follows: In the vicinity of the stagnation point at high Mach numbers, the shock shape and shock stand-off distance is nearly independent of the Mach number. Furthermore, the slope of the shock at the opposite extremity, i.e., the Mach line, does not differ greatly at high Mach numbers. Since both ends are nearly the same, one can expect only small variations in the shock shape with Mach number.

The curves of energy flux change show a peak near $\bar{y}_s = 1$, a sharp fall-off and a rather long tail. This means the high temperatures will occur near the body, but a good deal of the energy increase in the fluid occurs beyond $\bar{y}_s = 2$. Based on the area under the curves of Fig. 3, about 15% of the complete enthalpy change occurs within $\bar{y}_s = 1$, and approximately 40% of the change occurs within $\bar{y}_s = 2$. These percentages would be reduced somewhat if the missing portion of the shock shape was included.

The main source of error in the above calculation is the use of a shock shape for a semi-infinite hemisphere cylinder based on a Mach number lower than those used in the calculation. Both of these approximations tend to shift the energy distribution away from the body, but this shift is more than accounted for by the missing portion of the shock curve. For this reason, the percentages quoted above would appear to be qualitatively correct.

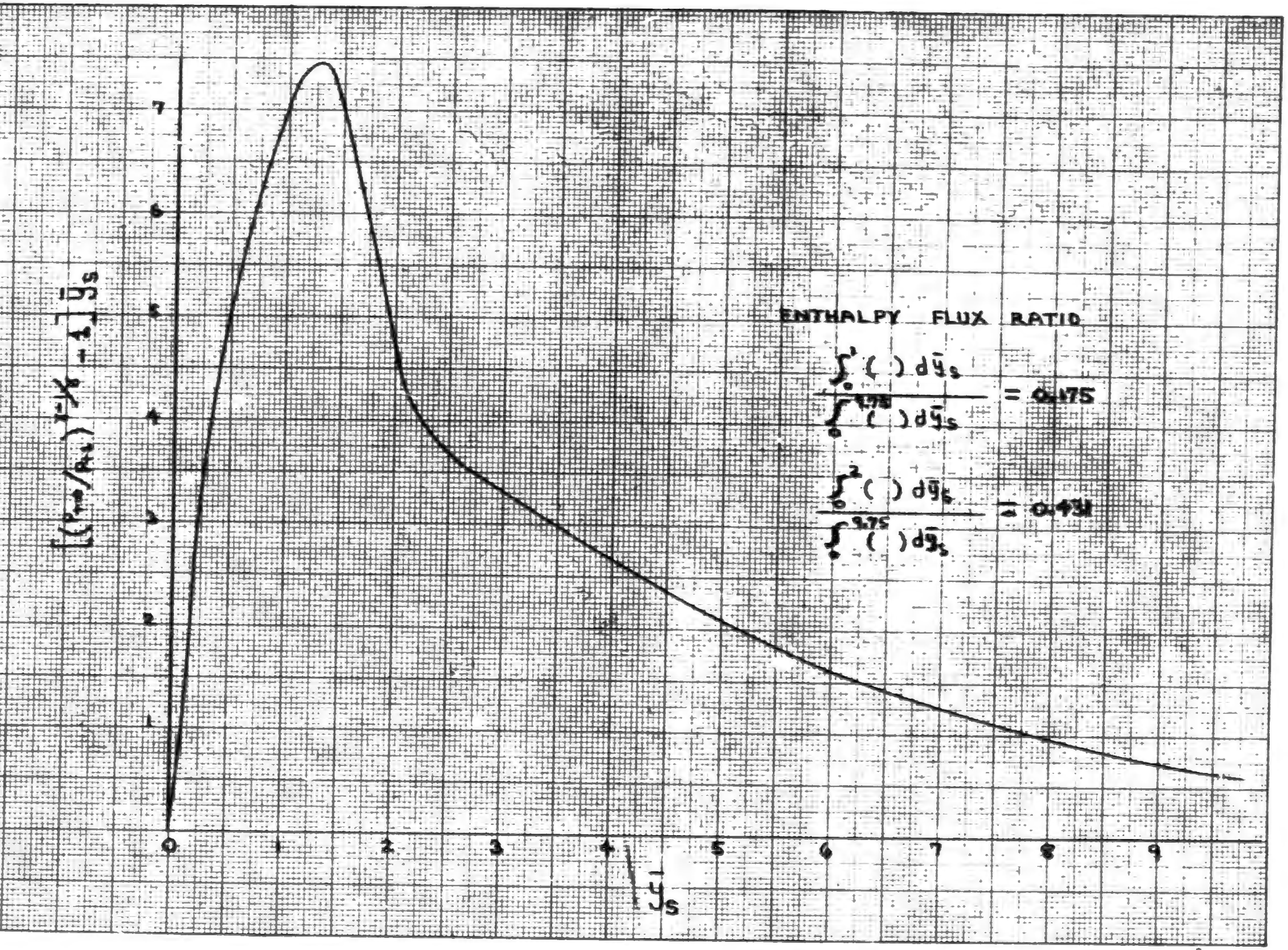

FIGURE 3: DISTRIBUTION OF THE CHANGE IN ENTHALPY FLUX

(a) $M_\infty = 20$

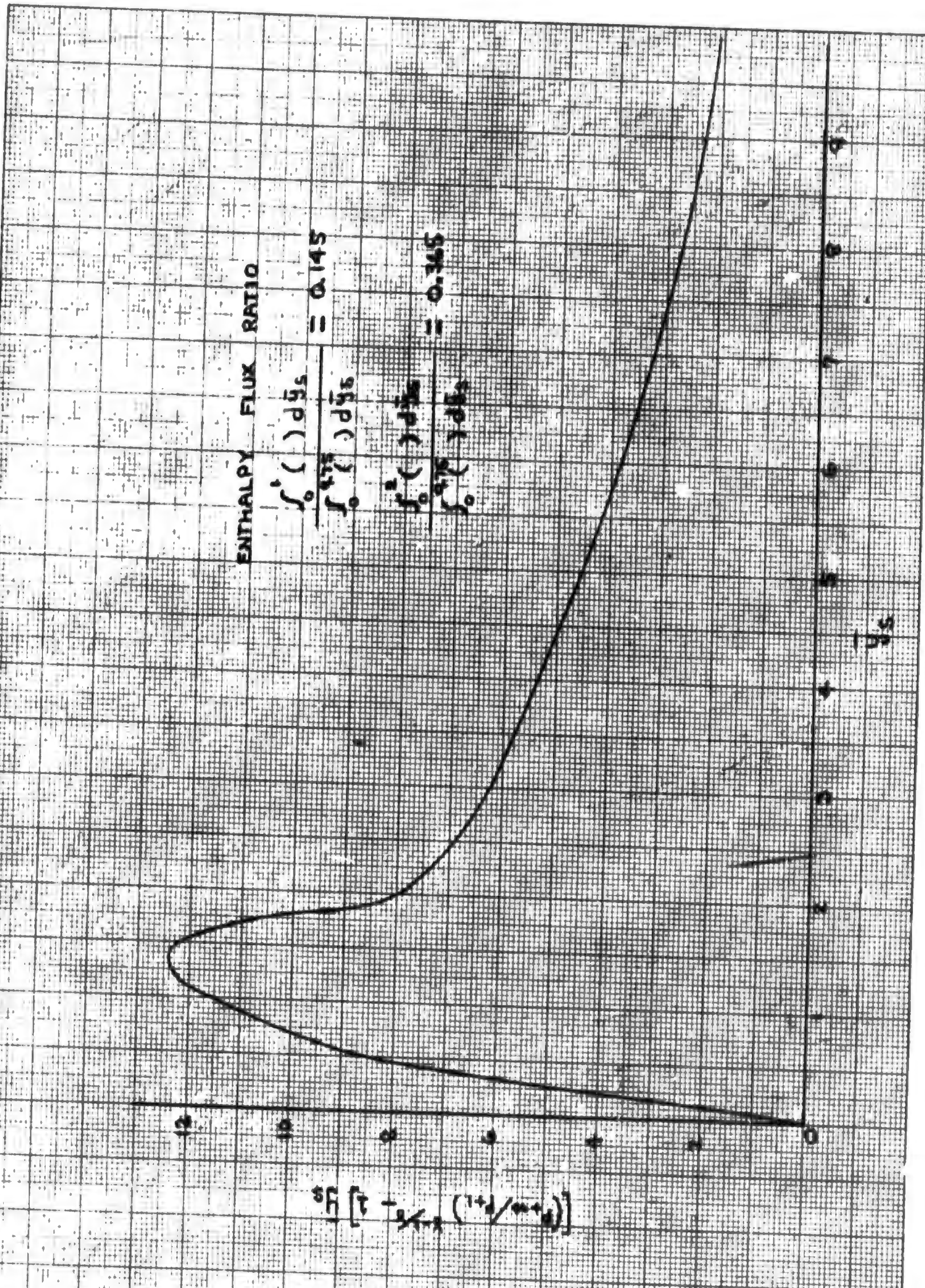

FIGURE 3: DISTRIBUTION OF THE CHANGE IN ENTHALPY FLUX

(b) $M_\infty = 27.7$

Conclusions

To attempt to further extend this analysis would require a knowledge of the true shock shape. However, this analysis does indicate that a large percentage of the energy increase behind a shock wave can occur outboard of 2 nose radii of the body. It also shows that a knowledge of the wave drag coefficient is sufficient to compute the rate of change of enthalpy of the entire flow field. These calculations provide, in a quantitative way, a means of estimating the energy distribution in the wake of re-entry bodies at relatively high altitudes.

References

1. Allen, H.J. and Eggers, A.J., Jr., A Study of the Motion and Aerodynamic Heating of Missiles Entering the Earth's Atmosphere at High Supersonic Speeds, NACA TN 4047, October 1957.

2 Feldman, Saul, Trails of Axi-symmetric Hypersonic Blunt Bodies Flying Through the Atmosphere, Avco Research Report 82, December 1959.

3. Munk, M.M. and Crown, J.C., The Head Shock Wave, NOL Memo 9773.

4. Sommer, S.C. and Stark, J.A., The Effect of Bluntness on the Drag of Spherical-Tipped Truncated Cones of Fineness Ratio 3 at Mach Numbers 1.2 to 7.4, NACA RM A52B13, 1952.